Pol. J. Environ. Stud. Vol. 31, No. 4 (2022), 3447-3454
DOI: *10.15244/pjoes/146008* ONLINE PUBLICATION DATE: 2022-05-02

Original Research

Adsorption Characteristics of Lead Ion by Sorghum Vinasse

Tao Zhao#, Guangqian Dai#, Hui Gu, Rongguo Sun*

School of Chemistry and Material, Guizhou Normal University, Guiyang 550025, China

Received: 28 October 2021
Accepted: 21 January 2022

Abstract

Laboratory experiments were designed to identify the adsorption features of Pb^{2+} by sorghum vinasse (SV) under various conditions. The results showed that the adsorption capacity enhanced with the increasing pH and peaked (68.42 ± 1.42 mg g^{-1}) when pH = 6. With the SV dosage ranging from 0.0250 to 0.2000 g, the adsorption capacity declined from 55.59 to 44.84 mg g^{-1}, and the Pb^{2+} removal rates increased from 13.52% to 91.14%. The adsorption capacity reached 95.4% of the maximum adsorption capacity at the 10th min, then rose slowly with respect to contact time and equilibrated at the 360th min. When the initial Pb^{2+} content < 400 mg L^{-1}, the adsorption capacity increased quickly, then it did not vary significantly with the increasing initial Pb^{2+} concentration. These suggest that the initial pH, adsorbent dosage, contact time, and the initial Pb^{2+} concentration can significantly affect the adsorption process. The pseudo-second-order kinetic and Langmuir model could well illustrate the adsorption process. The adsorption of Pb^{2+} on SV is a chemical and spontaneous process via monolayer adsorption involving physical absorption, ion exchange, surface complex with OFGs, and chemical reactions.

Keywords: lead, sorghum vinasse, adsorption, mechanism

Introduction

In recent years, with increasing human activities and the discharge of industrial sewage, heavy metal pollution in the water environment has become more and more serious [1]. Heavy metals have caused great harm to ecosystems and human bodies due to their self-toxicity and refractory properties. At present, the methods for treating heavy-metal-contaminated sewage include electro-coagulation, ion exchange, membrane filtration, and adsorption [2]. Among these methods adsorption has attracted much attention due to its simplicity, low cost, and efficiency for wastewater treatment, making it is the most economical solution [3].

Lead (Pb) is one of the heavy metals widely present in industrial effluents. Pb can be assimilated and concentrated in animal tissues via the food chain, then injure the nervous, blood, and digestive system [4]. Biochar, nanomaterials, and biomass waste have been used to adsorb Pb in aqueous solutions [5, 6]. The hydroxyl, carboxyl, carbonyl, alcohol, phenol, and other surface oxygen-containing functional groups (OFGs) contained in these biomass waste have a particularly high affinity for adsorbing Pb^{2+}. The adsorption

#Tao Zhao and Guangqian Dai are co-first authors and contributed equally to this work.Mailing address: University Town of Huaxi, Guian District, Guizhou, 550025, P.R. China
*e-mail: srg@gznu.edu.cn

mechanism involves physical and chemical adsorption, including surface adsorption, pore size diffusion, intermolecular force, ion exchange, functional group complex, and precipitation, etc. [7, 8]. At present, the sorbent preparation for adsorbing Pb^{2+} from biomass waste processing materials has become one of the research hotspots.

Sorghum vinasse (SV) is the final by-product of the grains (sorghum, corn, or wheat) distillation for ethanol production. The yield of SV is 3.0×10^7 tones of 2014 in China and shows an increasing tendency year by year [9]. Only a tiny amount of SV is disposed of feeding animals, while most SV are discarded with no management. This will cause serious environmental problems such as uncontrolled decomposition, rotting, fetor, spreading bacteria and viruses, and leakage of percolate. Therefore, appropriate reuse of SV will help for protecting the local environment, and contribute to the sustainable development of the liquor industry. There is plenty of organic matter, potassium ion, cellulose, hemicellulose, and lignin contained in SV [10], thus having abundant OFGs including carboxylate, aromatic carboxylate, phenolic hydroxyl, hydroxyl, etc. [11]. These OFGs have a particularly high affinity for binding heavy metal ions [11]. Therefore, it is speculated that SV has a specific adsorption performance for Pb ions, but the adsorption characteristics and mechanisms are currently unclear.

Given the above consideration, this study aims to (1) identify the adsorption behavior of Pb^{2+} by SV under the conditions with different solution pH, SV dosages, contact time, or initial Pb^{2+} concentrations, (2) elucidate the adsorption mechanism through analyzing the adsorption kinetics, isothermal adsorption model, and the roles of SV microstructure in adsorption processes. The results can provide research bases for SV applying in the processes of leaded wastewater decontamination.

Material and Methods

Chemicals and Materials

SV was obtained from a brewhouse located in Renhuai, Guizhou Province, China, the primary raw materials of which were sorghum and wheat. SV was ground and sieved to 100 mesh (0.15 mm) after washing with deionized water (resistivity >18.2 MΩ cm^{-1}), then dried at 80ºC to a constant weight. The standard reserving solution for Pb^{2+} was prepared by dissolving solid $Pb(NO_3)_2$ (GR, Guoyao, China) in deionized water (resistivity >18.2 MΩ cm^{-1}) to be 1000 mg L^{-1}, which is diluted to the required concentrations for experiments.

Experiment Design and Characterization Methods

According to the experiment design presented in Table 1, a certain amount of SV and leaden solution were orderly added into Teflon centrifuge tubes. Hydrochloric acid (1 M, GR, Guoyao, China) and sodium hydroxide solution (1 M, GR, Guoyao, China) were used to adjust the pH values. The Teflon centrifuge tubes (with cover) were placed on a thermostatic oscillation incubator and shaken at a constant speed (120 rpm) for 1440 min under the room temperature of 25ºC. Supernatants were extracted by centrifugation under 5500 r min^{-1} for 5 min, and carefully filtered with 0.25 μm polyvinylidene fluoride membrane (Millipore, USA). The flame atomic absorption spectrometry (Aanalyst 400, PerkinElmer, USA) was employed for determining the Pb^{2+} contents in supernatants. All adsorption experiments were conducted in triplicate. The triplicate analysis for all samples, certified reference material (GBW (E) 083779), and method blanks were completed for the quality assurance of analyzing Pb^{2+}. The detection limits were measured to be 0.01 mg L^{-1} for Pb^{2+} in solution. The method blanks were taken regularly with more than 15% of the total samples.

The surface morphology of the SV before and after adsorbing Pb^{2+} was characterized by scanning electron microscopy with an energy dispersive spectrometer (SEM-EDX, FEI Quanta 250 FEG, USA). The crystalline forms of chemical precipitates were determined by X-ray diffraction (XRD, Hermofisher K-Alpha, USA). The functional groups of SV were determined by fourier transform infrared spectroscopy (FTIR, FTIR-650, China). The surface area to volume ratio was determined by Brunauer-Emmett-Teller (BET,

Table 1. Details of experimental design.

Experimental No.	Investigate factor	Other factors	Objectives
1	pH = 2, 3, 4, 5, and 6	m [a] = 0.1 g, C_0 [b] = 400 mg L^{-1}, t [c] = 1440 min	Identify the effects of pH
2	m = 0.025, 0.05, 0.1, 0.15, and 0.2 g	C_0 = 400 mg L^{-1}, pH = 5 ± 0.03, t = 1440 mins	Clarify the effects of the SV dosage applied
3	t = 10, 30, 60, 120, 240, 360, 480, 720, and 1440 mins	m = 0.1 g, C_0 = 400 mg L^{-1}, pH = 5 ± 0.03, t = 1440 mins	Investigate the adsorption characteristics at various contact times
4	C_0 = 10, 50, 100, 200, 300, 400, 500, and 600 mg L^{-1}	m = 0.1 g, C_0 = 400 mg L^{-1}, pH = 5 ± 0.03, t = 1440 mins	Identify the effects of initial concentration of Pb^{2+}

Annotation: [a] m is the SV dosage, [b] C_0 is the initial concentration of Pb^{2+}, and [c] t is the contacting time.

Quantachrome NOVA1994-2007, UAS) under nitrogen atmosphere.

Data Analysis

The adsorption capacities and removal rate of Pb^{2+} adsorbed on SV were calculated using Eq. (1) and Eq. (2), respectively.

$$Q_e = \frac{V \times (C_0 - C_t)}{m} \quad (1)$$

$$W\% = \frac{C_0 - C_T}{C_0} \times 100\% \quad (2)$$

Where Q_e is the equilibrium adsorption capacity (mg g^{-1}); C_0 and C_t is the respective concentrations of Pb^{2+} at time 0 and t in supernatants (mg L^{-1}); V is the solution volume (L), m is the mass of adsorbent (g); $W\%$ is the removal rate of Pb^{2+}.

The Langmuir isotherm (Eq. (3)) and Freundlich isotherm (Eq. (4)) models were employed to simulate the sorption isotherms [12].

$$\frac{C_e}{Q_e} = \frac{1}{K_l Q_{max}} + \frac{C_e}{Q_{max}} \quad (3)$$

$$\log Q_e = \log K_f + \frac{1}{n} \log C_e \quad (4)$$

Where C_e is the equilibrium concentrations of Pb^{2+} (mg L^{-1}); Q_e and Q_{max} is the equilibrium and maximum adsorption capacity (mg g^{-1}), respectively; K_l and K_f is the Langmuir and Freundlich constant, respectively.

Pseudo-first-order (Eq. (5)) and Pseudo-second-order (Eq. (6)) kinetic models were both applied to analyze the sorption kinetics of Pb^{2+} on SV [12].

$$\ln(Q_e - Q_t) = \ln Q_e - K_1 t \quad (5)$$

$$\frac{t}{Q_t} = \frac{1}{K_2 Q_e^2} + \frac{t}{Q_e} \quad (6)$$

Where t is the adsorption time (min); Q_e is the equilibrium adsorption capacity (mg g^{-1}); Q_t is the adsorption capacity at time t (mg g^{-1}); K_1 and K_2 is the Pseudo-first-order and Pseudo-second-order rate constant, respectively.

Results and Discussion

Effects of Initial pH

The adsorption capacity for Pb^{2+} on SV was 5.55±1.49 mg g^{-1} when pH = 2, then it increased with the increasing pH and reached a maximum value of 68.42±1.42 mg g^{-1} when pH = 6 (Fig. 1a). This suggests that the initial pH plays a key role in affecting the adsorption process of Pb^{2+} on SV. It had reported that the initial pH of the reaction solution could significantly influence the adsorption capacity of metals on absorbents via the pathways affect the distribution

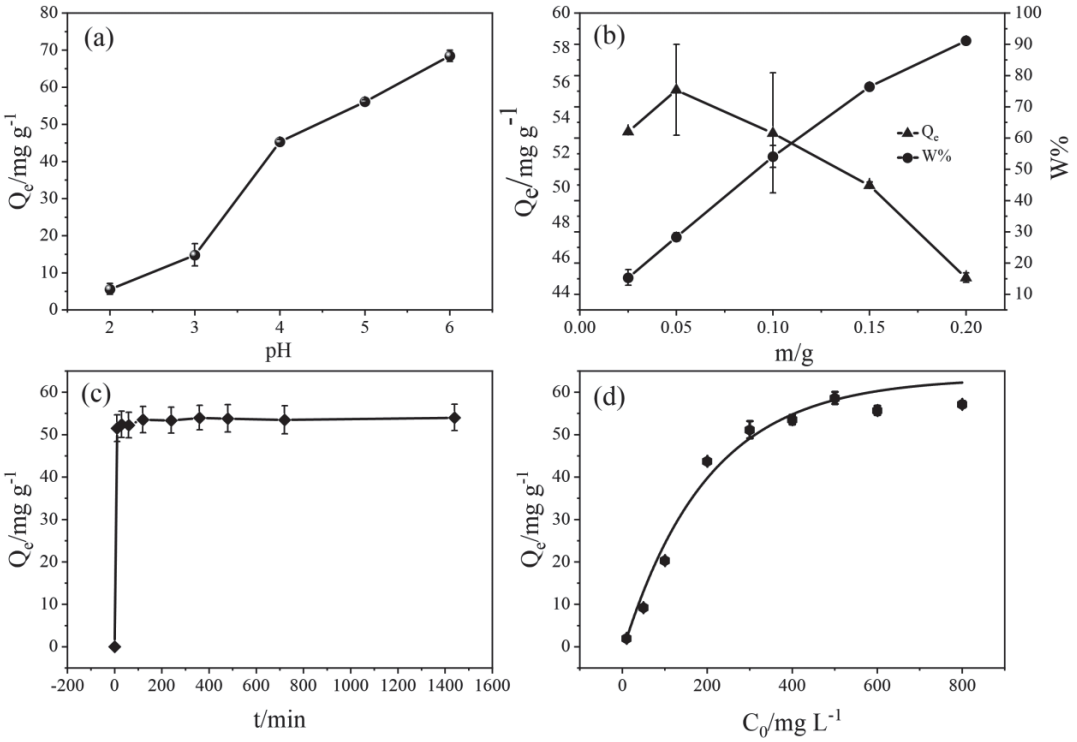

Fig. 1. Influences of solution pH a), SV dosage b), contact time c), and initial Pb^{2+} concentration d) on adsorbtion process.

of surface charge and the speciation of heavy metals in the solution [13]. There were large amounts of H^+ in the reaction solution when pH = 2-4. The H^+ was adsorbed onto the SV surface and competed with Pb^{2+}, resulting in the adsorption of Pb^{2+} on SV being inhibited. With the initial pH value of the reaction solution increased, the H^+ amount in the solution decreased simultaneously; thus the surface OFGs of SV become deprotonated, which is more favorable for binding Pb^{2+}. When the pH>5, the Pb^{2+} would coordinate with hydroxyl ion (OH-), then $Pb(OH)^+$ and $Pb_2(OH)^{3+}$ were formed, which could enhance the adsorption of Pb^{2+} on SV. The precipitates, $Pb(OH)_2$, could be generated and adsorbed onto SV when the pH≥6, causing the adsorption capacity of Pb^{2+} on SV to increase significantly. Under the natural aquatic environment, Pb^{2+} and $Pb(OH)^+$ are the dominate species of Pb when pH≤5.5, and $Pb(OH)_2$ is generated when pH = 5.5-12.5 [14,15]. The coordination of Pb^{2+} with OH- can decrease the concentration of free Pb^{2+} in solution. Thereby, the real adsorption capacity of Pb^{2+} on SV is difficult to estimate. Therefore, for avoiding the influence of the coordination of Pb^{2+} with OH- and generating precipitation, pH = 5 was determined as the optimal value for researching the adsorption processes of Pb^{2+} on SV.

Effects of Adsorbent Dosage

With the SV dosages ranging from 0.0250 to 0.2000 g, the adsorption capacity of Pb^{2+} on SV decreased from 55.59 to 44.84 mg g^{-1}, and the removal rates of Pb^{2+} increased from 13.52% to 91.14% (Fig. 1b). With the increasing of the SV dosage, the adsorption site increased simultaneously, while the initial Pb^{2+} concentrations were constant, resulting in the adsorption processes changing from saturation to unsaturation [16, 17]. Therefore, the SV dosage has significant effects on the adsorption processes.

Effects of Contact Time

The contact time had essential effects on the adsorption process of Pb^{2+} on SV (Fig. 1c). The adsorption capacity of Pb^{2+} on SV was calculated to be 51.47 mg g^{-1} at the 10^{th} min, which was 95.4% of the maximum adsorption capacity (53.95±2.88 mg g^{-1}). Then the adsorption capacity increased slowly concerning contact time and reached equilibrium at the 360^{th} min. The removal rate of Pb^{2+} in equilibrium was 53.96%. These results indicate that Pb^{2+} is quickly adsorbed via physical adsorption once the SV is added into the reaction solution. The total active adsorption sites on SV were constant when 0.1 g of SV was spiked into the reaction mixture. It's hypothesized that each active site can absorb one Pb^{2+} via monolayer adsorption. Thereby, the adsorption processes will be quickly within 10 min. Then the number of active adsorption sites decreased with reaction time, resulting in the adsorption rates decreased. In the present study, the adsorption capacity was calculated based on the concentrations of Pb^{2+} in the reaction solutions. Actually, they are net results because the adsorption and desorption processes co-occur. Although the adsorption processes had approximately reached the equilibrium at the 360^{th} min, the 1440^{th} min was chosen as the optimum contact time in all experiments to research the adsorption characteristics because it should be assured that the adsorption and desorption processes completely reached the equilibrium.

Effects of Initial Pb^{2+} Concentration

As the increasing of initial Pb^{2+} concentrations, the equilibrium adsorption capacity of Pb^{2+} on SV could be divided into two phases (Fig 1d). The first phase was when the initial Pb^{2+} concentrations <400 mg L^{-1}, the adsorption amount of Pb^{2+} enhanced quickly as the increasing initial Pb^{2+} concentration. The SV can provide enough active adsorption sites for absorbing Pb^{2+}; consequently, the equilibrium adsorption capacity of Pb^{2+} on SV increased with increasing initial Pb^{2+} concentrations. Therefore, the initial Pb^{2+} concentration is the main factor affecting adsorption process at this phase. When the initial Pb^{2+} concentrations surpassed 400 mg L^{-1}, the active adsorption sites for absorbing Pb^{2+} were occupied completely, showing that the adsorption capacities reached equilibrium. During the adsorption processes, different Pb^{2+} concentrations could provide various driving forces to surmount the resistance between the solid and liquid phases [15]. Therefore, the slowly increasing adsorption capacity at high initial Pb^{2+} concentration can be attributed to the elevated driving forces between the solid and liquid phase provided by Pb^{2+}, which inhibit the adsorption process [18].

Adsorption Kinetics

According to the coefficient of determination (R^2 = 0.99, Fig. 2(a-b)), the adsorption kinetics of Pb^{2+} on SV could be well illustrated by the pseudo-second-kinetic model. Besides, the theoretical adsorption capacity (53.99 mg g^{-1}) obtained from the pseudo-second-order kinetic model is approximately equal to the experimental data. This means that the adsorption of Pb^{2+} on SV may be a chemical process, which is involved in affecting valence force via sharing or exchange of electrons between SV and Pb^{2+} [19].

Sorption Isotherms

The sorption isotherms and possible adsorption mechanism were described by Langmuir and Freundlich isothermal adsorption model (Fig. 2(c-d)). The modeling maximum adsorption capacity (62.66 mg g^{-1}) obtained from the Langmuir model was close to the experimental data (57.13 mg g^{-1}). In addition, the coefficient of determination from the Langmuir model (R^2 = 0.98) was much higher than that from the Freundlich model

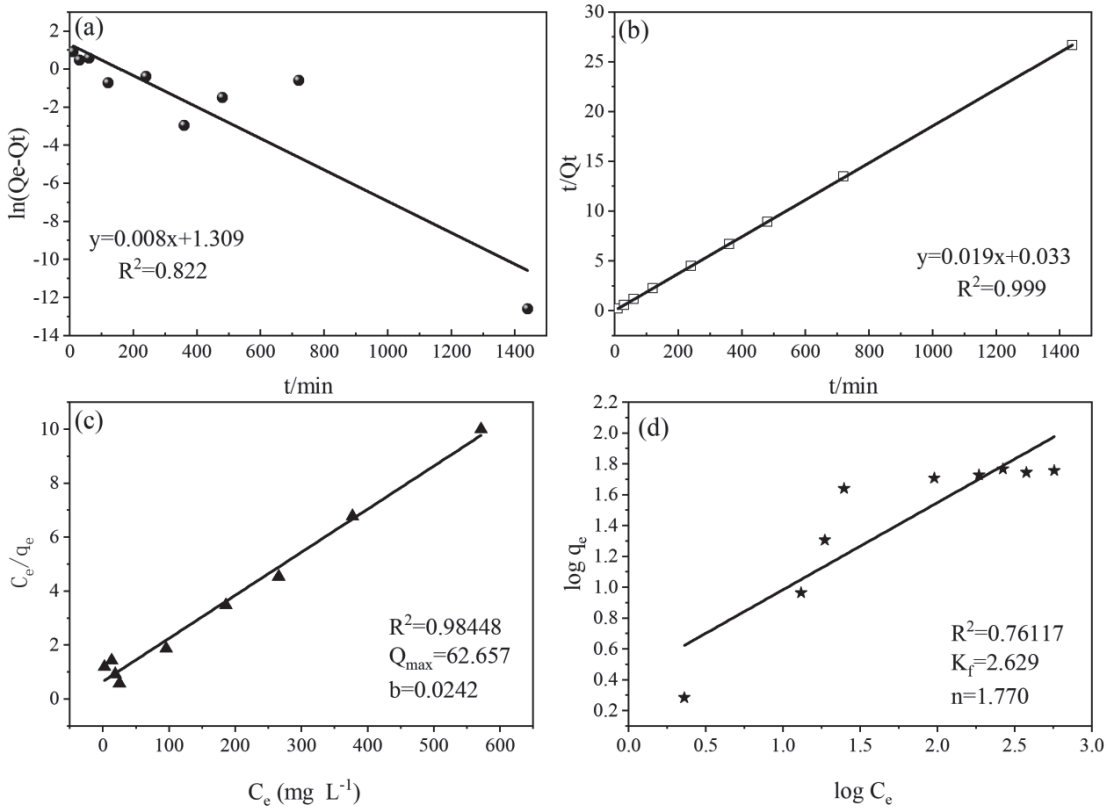

Fig. 2. The fitting results of the pseudo-first-order a), pseudo-second-order kinetic b), Langmuir c), and Freundlich d) models of SV adsorbing Pb^{2+}.

(R^2 = 0.76), suggesting that the adsorption process of Pb^{2+} on SV was better illustrated by the Langmuir model. This demonstrated that the adsorption process of Pb^{2+} on SV was mainly monolayer adsorption [20].

Rise of the Microstructure of SV in Adsorption Processes

The surface area to volume ratio and porosity is the dominant physical properties that can affect the adsorption capacity of metals by absorbents. The surface micrographs of SV display a fine claviform structure with inner porosity, and the surface area to volume ratio is 1.602 m^2 g^{-1}. After the SV adsorbed Pb^{2+}, the fine claviform became coarse and piled layered on the surface of SV (Fig 3). The inner porosity was disappeared, and the surface area to volume ratio was 3.294 m^2 g^{-1}. The increasing of surface area to volume ratio might be attributed to that Pb^{2+} was adsorbed on the surface and inner porosity, resulting in the inner porosity being blocked. Consequently, the surface area to volume ratio increased after adsorption, which meant that the physical absorptions occurred during the adsorption process.

The EDX spectra show that alkali metals (K, Ca, Na, Mg) can be detected before adsorbing Pb^{2+} (Fig. 3a), and cannot be detected after adsorption (Fig. 3b), demonstrating that the alkali metals are released during the adsorption process. This is mainly caused by that alkali metals have high activity and mobility, and can be exchanged with Pb^{2+} as Eqs (7) and (8) [21]. Therefore, we can conclude that ion-exchange between alkali metals and Pb^{2+} are involved in the adsorption process.

$$SV\text{-}Ca^{2+} + Pb^{2+} \rightarrow SV\text{-}Pb^{2+} + Ca^{2+} \quad (7)$$

$$SV\text{-}Mg^{2+} + Pb^{2+} \rightarrow SV\text{-}Pb^{2+} + Mg^{2+} \quad (8)$$

Before absorbing Pb^{2+}, the characteristic diffraction peaks of SiO_2 (2θ = 20.6°, 26.3°, 50.1°, and 59.8°) and $CaAl_2SiO_8 \cdot 4H_2O$ (2θ = 26.4°, 28.9°, 36.3°, 42.6°, 50.3°, and 60°) were observed. After loading with Pb^{2+}, the intensities of diffraction peaks at 26.3° decreased significantly, and the characteristic diffraction peaks of $CaAl_2SiO_8 \cdot 4H_2O$ were not observed. Meanwhile, a new characteristic diffraction peak of $Pb(ClO_4) \cdot 3H_2O$ (2θ = 30.3°) was found (Fig. 4a). It had been reported that Pb^{2+} could be removed by absorbent through surface precipitation because Pb^{2+} could react with H_2O and CO_2 to generate PbO, $PbCO_3$, and $Pb(OH)_2$ [22]. In the present study, XRD analysis did not find these species of Pb, which suggested PbO, $PbCO_3$, and $Pb(OH)_2$ were not formed and deposited on the surface of SV under acidic conditions (pH = 5). By combining these results with the EDX spectra, it was concluded that surface

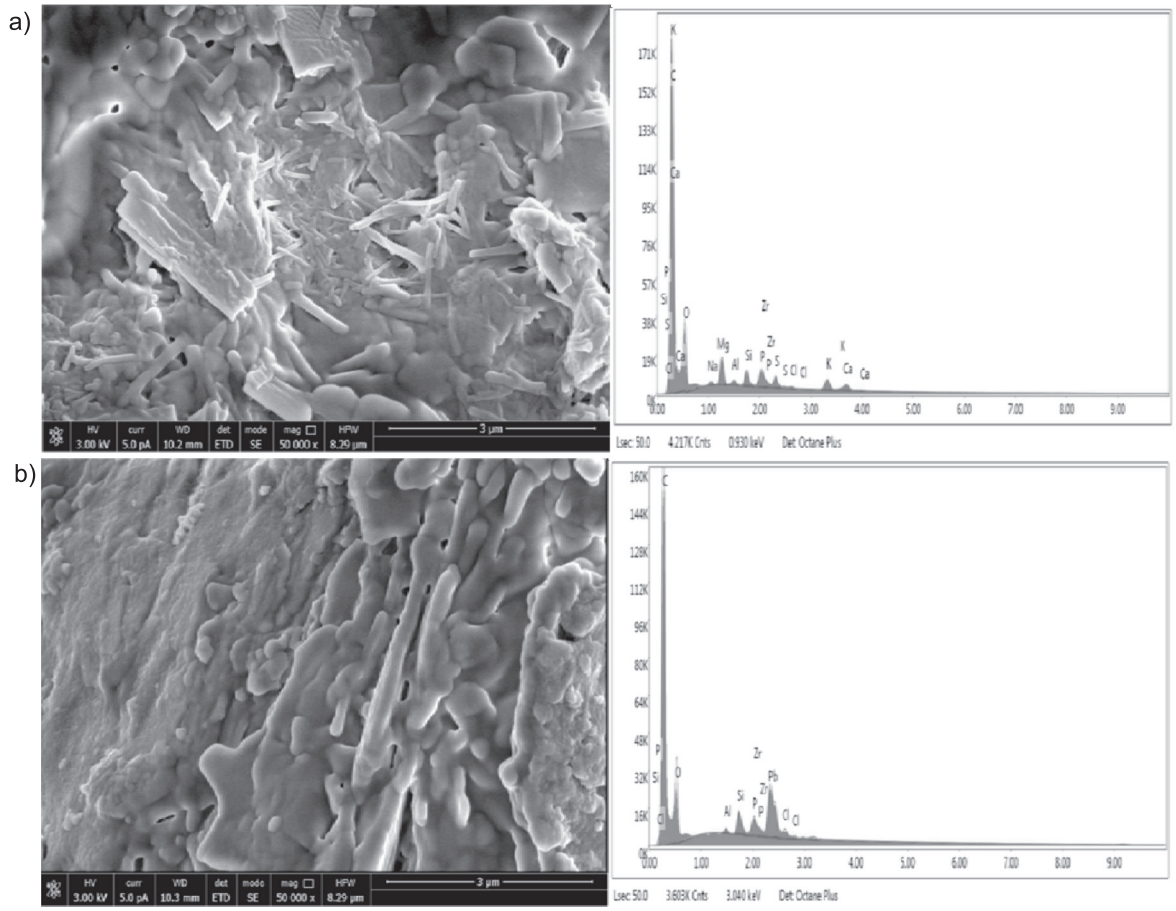

Fig. 3. The SEM and EDX of SV before a) after b) absorbing Pb^{2+}.

precipitation was not the governing mechanism for removing Pb^{2+} by SV, and the predominant pathway was ion exchange.

The OFGs, including acidic group, carboxyl, and hydroxyl on the adsorbent surface, can be complexed with Pb^{2+}, which is of great importance for absorbing Pb^{2+} [23]. FTIR spectroscopy was thus recorded (Fig. 4b) to identify the change of OFGs of SV before and after absorbing Pb^{2+}. In the spectrum of SV before absorbing Pb^{2+}, the band at 3334 cm^{-1} was assigned to the structural -NH_2 and -OH stretching vibration, which appeared in low intensity after absorbing Pb^{2+} [24]. This was caused by that Pb^{2+} superseded -H in these OFGs, revealing that ion exchange was presented in the adsorption process (Eq. (9)). As for SV, before absorbing Pb^{2+}, the absorption at 2925 and 2852 cm^{-1} came from the stretching vibration of -CH_3 and -CH_2 (the characteristic absorption of methyl and methylene),

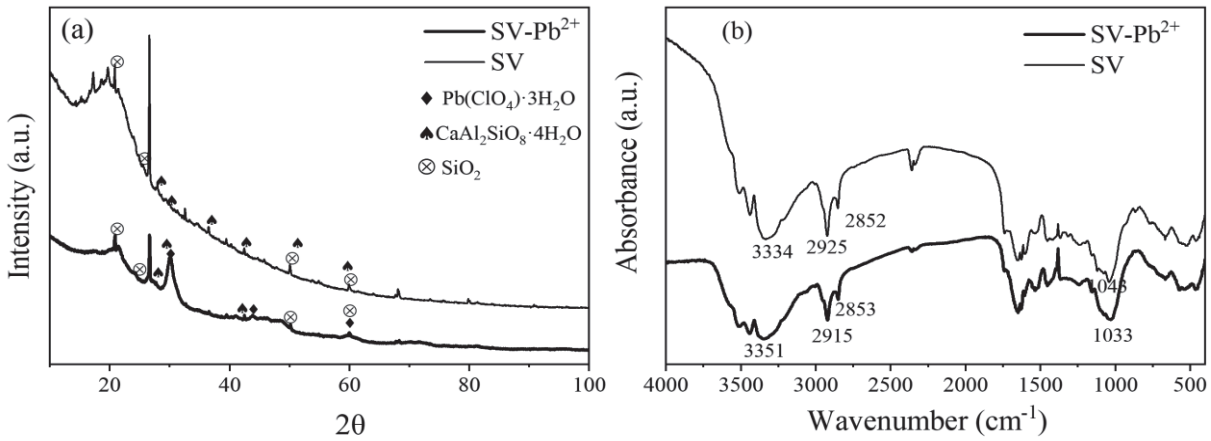

Fig. 4. The XRD a) and FTIR b) of SV before and after absorbing Pb^{2+}.

Table 2. Adsorption characteristics of Pb(II) by various absorbents existing in the literature.

Absorbent	Sorption isotherms	Adsorption kinetic	Q/(mg g^{-1})	Reference
SV	Langmuir	the Pseudo-second-order	52.51	The present study
Corn stalk	Freundlich	the Pseudo-second-order	90.00	[27]
Hazelnut husk	Langmuir	-	28.18	[6]
Almond husk	Langmuir	-	8.08	[6]
Watermelon residue	Langmuir	the Pseudo-second-order	24.15	[28]
Watermelon residue	Langmuir	the Pseudo-second-order	116.20	[29]
Grape stalk	Langmuir	the Pseudo-second-order	49.94	[30]

respectively. After absorbing Pb^{2+}, these vibrations shifted to 2925 and 2853 cm^{-1}, suggesting that chemical reactions were involved in adsorption processes. The C=O stretching vibration in carboxylic acid at 1741 cm^{-1} and $-COO^-$ antisymmetric stretching vibration in organic carboxylate at 1654 cm^{-1} decreased drastically after absorbing Pb^{2+}. This is caused by that carboxyl groups on the surface of SV can react with Pb^{2+} to generate SV-CO-Pb^+ and $(SV\text{-}CO)_2Pb$ as Eqs (10) and (11) [25]. The adsorption at 1043 cm^{-1} came from the stretching vibration of Si-O, the intensity of which decreased after absorbing Pb^{2+}. This implies that SiO_2 has a strong affinity to Pb^{2+}, which is similar to the previous study [26]. These FTIR analyses indicated that the hydroxyl group (-OH), amino group ($-NH_2$), carboxyl functional group (-COOH), and other aromatic groups from cellulose, lignin, and semi-fiber on the surface of SV can absorb Pb^{2+} through complexation. Based on the above analysis, it can be seen that the adsorption of Pb^{2+} on SV mainly via physical absorption, ion exchange, surface complex with OFGs, and chemical reactions.

$$(SV\text{-}OH)_2 + Pb^{2+} \rightarrow (SV\text{-}O)_2Pb + 2H^+ \quad (9)$$

$$SV\text{-}COOH + Pb^{2+} \rightarrow SV\text{-}CO\text{-}Pb^+ + H^+ \quad (10)$$

$$(SV\text{-}COOH)_2 + Pb^{2+} \rightarrow (SV\text{-}CO)_2Pb + 2H^+ \quad (11)$$

Comparison of Adsorption Characteristics of Pb(II) by Various Absorbents

The isothermal adsorption model, kinetics, and adsorption capacity by various absorbents are summarized in Table 2. The Langmuir adsorption model can well illustrate the adsorption processes of Pb^{2+} by different biosorbents, suggesting that the adsorption process of Pb^{2+} by different biosorbents are mainly monolayer adsorption. The adsorption kinetics of Pb^{2+} by different biosorbents can be described by the pseudo-second-order kinetic. This indicates that the adsorption of Pb^{2+} by biosorbent is a chemical process, which is involved in affecting valence force via sharing or exchange of electrons between biosorbents and Pb^{2+}. The biosorbent, SV, is neither the best nor the worst because the adsorption capacity of Pb^{2+} on SV we obtained is within the general broad reported by others. This implies that the SV has a particular application prospect in Pb cations removal of wastewater.

Conclusions

Sorghum vinasse (SV) is applied as biosorbents for removing the Pb^{2+} in aqueous solutions. The adsorption Pb^{2+} on SV can be significantly affected by the solution's initial pH, SV amount, reaction time, and the initial Pb^{2+} concentration. The adsorption of Pb^{2+} on SV is a quick and physical process. The adsorption capacity of Pb^{2+} on SV increased simultaneously with the increasing of the initial solution pH. In contrast, the adsorption capacity of Pb^{2+} on SV decreased with increase SV dosage. The adsorption capacity increased quickly when the initial Pb^{2+} concentrations were lower than 400 mg L^{-1}, then it did not vary significantly with the increasing initial Pb^{2+} concentrations.

The adsorption process of Pb^{2+} on SV can be well illustrated by the pseudo-second-order kinetic model, indicating that the adsorption of Pb^{2+} on SV is a chemical process. The Langmuir model can well illustrate the adsorption process of Pb^{2+} on SV, suggesting that the adsorption process of Pb^{2+} on SV is mainly monolayer adsorption and a spontaneous process. The SEM, EDX, XRD, and FTIR were employed to investigate the adsorption mechanism of Pb^{2+} on SV. Overall, the adsorption of Pb^{2+} on SV occurs mainly via physical absorption, ion exchange, surface complex with OFGs, and chemical reactions.

Acknowledgments

This work was financially supported by the Science and Technology Department of Guizhou Province (No. Qian ke he ji chu [2020]1Z038), the Doctoral Scientific Research Foundation of Guizhou Normal University for 2014 (No. 11904/0514154), and the Postgraduate Scientific Research Foundation of Guizhou Province (Qian Jiao He YJSCXJH [2020]101).

Conflict of Interest

The authors declare no conflict of interest.

References

1. ZHANG Z.J., LI D.H., XU Z.G. Present Conditions、Reasons and Measures of Lead Pollution in China. Environmental Protection Science, **31** (130), 42, **2005**.
2. GUYO U., MHONYERA J., MOYO M. Pb(II) adsorption from aqueous solutions by raw and treated biomass of maize stover-A comparative study. Process Safety and Environmental Protection, **93**, 2, **2015**.
3. FAROOQ U., KOZINSKI J.A., KHAN M.A., ATHAR M. Biosorption of heavy metal ions using wheat based biosorbents-A review of the recent literature. Bioresource Technology, **101** (14), 5044, **2010**.
4. YANG Q.W., SHU W.S., QIU J.W., WANG H.B., LAN C.Y. Lead in paddy soils and rice plants and its potential health risk around Lechang lead/zinc mine, Guangdong, China. Environment International, **30** (7), 883, **2004**.
5. FU W., HUANG Z.Q. Magnetic dithiocarbamate functionalized reduced graphene oxide for the removal of Cu(II), Cd(II), Pb(II), and Hg(II) ions from aqueous solution: Synthesis, adsorption, and regeneration. Chemosphere, **209**, 450, **2018**.
6. PEHLIVAN E., ALTUN T., BHANGER M.I. Lead sorption by waste biomass of hazelnut and almond shell. Journal of Hazardous Materials, **167** (1), 1203, **2009**.
7. LU H.L., ZHANG W.H., YANG Y.X., HUANG X.F., WANG S.Z., QIU R.L. Relative distribution of Pb^{2+} sorption mechanisms by sludge-derived biochar. Water Research. **46** (3), 855, **2012**.
8. WANG Z.Y., LIU G.C., ZHENG H., LI F.M., NGO H.H., GUO W.S., LIU C., CHEN L., XING B.S. Investigating the mechanisms of biochar's removal of lead from solution. Bioresource Technology, **177**, 309, **2015**.
9. MA W.P., PEI F.X., REN H.W., XING J.M., ZHANG Y., ZHANG B.Y. Research Progress in Pretreatment Methods for Saccharification & Degradation of Distillers Grains. Liquor-Making Science & Technology, **258** (12), 90, **2015**.
10. KAZAK O., EKER Y.R., BINGOL H., TOR A. Preparation of chemically-activated high surface area carbon from waste vinasse and its efficiency as adsorbent material. Journal of Molecular Liquids, **272**, 189, **2018**.
11. BROWN P.A., GILL S.A., ALLEN S.J. Metal removal from wastewater using peat. Water Research, **34** (16), 3908, **2000**.
12. TRAN L., WU P.X., ZHU Y.J., LIU S., ZHU N.W. Comparative study of Hg (II) adsorption by thiol-and hydroxyl-containing bifunctional montmorillonite and vermiculite. Applied Surface Science, **356**, 97, **2015**.
13. WANG G.Y., ZHANG S.R., YAO P., CHEN Y., XU X.X., LI T., GONG G.S. Removal of Pb(II) from aqueous solutions by Phytolacca americana L. biomass as a low cost biosorbent. Arabian Journal of Chemistry, **11** (1), 103, **2018**.
14. TIWARI D., C. LALDANWNGLIANA, CHOI C.H., LEE S.M. Manganese-modified natural sand in the remediation of aquatic environment contaminated with heavy metal toxic ions. Chemical Engineering Journal, **171** (3), 963, **2011**.
15. HE H., ZHU Z.Q., LIU J., ZHU Y.N., YAN Q.M., LIU Y., MO N., XUAN H.L., WEI W.Y. Removal of Pb2+ from Aqueous Solution by Magnesium-Calcium Hydroxyapatite Adsorbent. Environmental Science, **40** (9), 4083, **2019**.
16. VERMA A., KUMAR S., KUMAR S. Statistical modeling, equilibrium and kinetic studies of cadmium ions biosorption from aqueous solution using S.filipendula. Journal of environmental chemical engineering, **5** (3), 2295, **2017**.
17. QU J.H., MENG X.L., JIANG X.Y., YOU H., WANG P., YE X.Q. Enhanced removal of Cd(II) from water using sulfur-functionalized rice husk: Characterization, adsorptive performance and mechanism exploration. Journal of Cleaner Production, **183** (10), 883, **2018**.
18. WANG Y.X., WANG H., LU P. Adsorption and kinetics of heavy metal (Zn) over biochars in solution. Chemical Industry and Engineering Progress, **38** (11), 5147, **2019**.
19. HO Y.S., G. MCKAY. Pseudo-second order model for sorption processes. Process Biochemistry, **34** (5), 452, **1999**.
20. WEI J.W., WEI Z.Z., LIAO L., ZHAO S.S., WANG D.Q. Aqueous Pb (II) removal adsorption on amine-functionalized mesoporous silica SBA-15. Chinese Journal of Environmental Engineering, **8** (5), 1829, **2014**.
21. BASU M., K. GUHA A., RAY L. Adsorption of Lead on Cucumber Peel. Journal of Cleaner Production, **151** (10), 610, **2017**.
22. WANG H.J., ZHOU A.L., PENG F., YU H., YANG J. Mechanism study on adsorption of acidified multiwalled carbon nanotubes to Pb(II). Journal of Colloid and Interface Science, **316** (2), 281, **2017**.
23. YANG X.P., CUI X.N. Adsorption characteristics of Pb (II) on alkali treated tea residue. Water Resources and Industry, **3**, 8, **2013**.
24. LIU J.Q., GUO J., WU A.L., DONG E.W., WANG J.S., WANG L.G., JIAO X.Y. Study on Infrared Spectroscopy of Decomposition Process of Sorghum and Corn Straw. Journal of Shanxi Agricultural Sciences, **47** (03), 391, **2019**.
25. WANG H.J., ZHOU A.L., PENG F., YU H., YANG J. Mechanism study on adsorption of acidified multiwalled carbon nanotubes to Pb(II). Journal of Colloid and Interface Science, **316** (2), 278, **2007**.
26. CHEN Z.M., FANG Y., XU Y.L., CHEN B.L. Adsorption of Pb^{2+} by rice straw derived-biochar and its influential factors, **32** (04), 775, **2012**.
27. JELENA T.P., MIRJANA D.S., JELENA V .M., MARIJA S.P., TATJANA D., MILA D.L., MARIJA L.M. Alkali modified hydrochar of grape pomace as a perspective adsorbent of Pb2+ from aqueous solution. Journal of Environmental Management, **182** (1), 297, **2016**.
28. AKKAYA G., GUZEL F. Bioremoval and recovery of Cu (II) and Pb (II) from aqueous solution by a novel biosorbent watermelon (Citrullus lanatus) seed hulls: kinetic study, equilibrium isotherm, SEM and FTIR analysis [J]. Desalination and Water Treatment, **51**, 7318, **2013**.
29. R. LAKSHMIPATHY., SARADA N.C. Metal ion free watermelon (Citrullus lanatus) rind as adsorbent for the removal of lead and copper ions from aqueous solution. Desalination and Water Treatment, **57** (33), 5, **2016**.
30. MARTINEZ M., MIRALLES N., HIDALGO S., FIOL N., VILLAESCUSA I., POCH J. Removal of lead (II) and cadmium (II) from aqueous solutions using grape stalk waste. Journal of Hazardous Materials, **133**, 207, **2006**.